Temperature and Gate Voltage Dependent Raman Spectra of Single-Layer Graphene

Khoi T. Nguyen, Daner Abdula, Cheng-Lin Tsai, and Moonsub Shim*

Department of Materials Science and Engineering, University of Illinois, Urbana, Illinois 61801, United States

ABSTRACT Raman spectra of electrostatically gated single-layer graphene are measured from room temperature to 560 K to sort out doping and thermally induced effects. Repeated heating cycles under Ar led to convergent first-order temperature coefficients of the G-band (χ_G = -0.03 cm^{-1}/K) and the 2D-band (χ_{2D} = -0.05 cm^{-1}/K) frequencies, which are independent of doping level as long as the Fermi level does not shift with temperature. While the intrinsic behavior may be different (*e.g.*, $\chi_G \sim -0.02$ cm^{-1}/K near room temperature), these values appear more appropriate in describing responses of most graphene samples on SiO_2 substrates. The more negative χ_G value than theoretical expectations may be explained by interactions with the substrate reducing the lattice thermal expansion contribution to the temperature dependence of G-band frequency. Enhanced interactions with the substrate may also be responsible for zero-charge, room-temperature G-band line width increase and 2D-band frequency downshift.

KEYWORDS: graphene · electrostatic gating · Raman spectroscopy · thermometry · substrate

Exceptionally high carrier mobilities and thermal conductivity observed in single-layer graphene have generated much excitement in multiple areas including low-dimensional physics, high-speed electronics, and thermal management applications.[1−3] Central to most electronics applications is the understanding and controlling doping/charging and thermal responses. Raman spectroscopy has been a powerful characterization tool for graphene and related materials especially with respect to doping and thermometry.[4−13] For example, Fermi level dependent electron−phonon coupling arising from the Kohn anomaly, "charge impurities", and heat dissipation processes in graphene have been examined with the aid of Raman spectroscopy.[5,6,9,14] In particular, changes in the G-band optical phonon energy and line width as well as G/2D intensity ratio have been frequently used to estimate doping levels and to infer temperature in graphene.[3,5,6,15] There are two key underlying physical processes that allow such measurements. Strong coupling of G-band phonons to carrier single particle excitations leads to phonon softening and broadening near the charge neutrality point or the Dirac point (DP).[16] Hence the G-band phonon energy and line width are strongly dependent on the Fermi level position or doping. With respect to heating when the Fermi level position is fixed at the DP, the decrease in the G-band line width is also dominated by the same electron−phonon coupling process, that is, thermal smearing of electron population distribution near the DP reducing the degree of electron−hole pair generation that is coupled to the optical phonon transition.[17] The downshift in the G-band phonon energy with increasing temperature, on the other hand, is dictated by anharmonic coupling mainly to acoustic phonons rather than electron−phonon coupling.[16,17] This downshift in the G-band phonon energy with temperature has often been used to estimate the temperature of graphene which has allowed for the use of Raman spectroscopy as a simple yet elegant means of studying thermal conductivity[3,7,18] and energy dissipation in graphene.[9,19] However, the effects of the local chemical environment, especially with respect to interactions with ambient molecules and substrates that can lead to charging, can complicate the interpretation of the temperature dependence of the Raman G-band energy and line width. Here, we examine Fermi level position dependent Raman spectra of single-layer graphene with varying temperature to separate out doping and temperature-induced effects.

RESULTS AND DISCUSSION

Raman spectra of electrically contacted graphene at the indicated temperatures with applied gate voltage (V_g) ensuring Fermi level position to be at the DP are shown in Figure 1. As expected, both the G and 2D modes downshift with increasing temperature. However, this temperature dependence can be significantly different when the Fermi level position is not ensured to be the same. Figure 2a shows V_g dependence

* Address correspondence to mshim@illinois.edu.

Received for review April 29, 2011 and accepted May 18, 2011.

Published online May 18, 2011
10.1021/nn201580z

© 2011 American Chemical Society

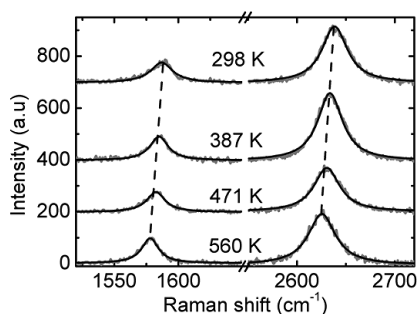

Figure 1. Raman G-band and 2D-band spectra of graphene at the indicated temperatures with the Fermi level fixed near the DP by applied gate voltage. Frequency downshift is indicated by the dashed line for both features. Solid black lines are Lorentzian curve fits. Spectra are offset for clarity.

of G-band frequency at different temperatures during the first heating cycle in Ar. The softening of G-band phonons near the DP due to the presence of the Kohn anomaly can be observed at all four temperatures. However, V_g corresponding to the DP at room temperature is different than at higher temperatures. The DP already shifts by -20 V even at a relatively low temperature of 387 K. Concurrent negative shift in the conductance minimum in the transfer characteristics can be seen in Figure 2b. Both of these results indicate the removal of hole doping effects[20,21] upon initial heating. The negative shift of 20 V for V_g at which the DP is observed corresponds to hole density decrease of 1.4×10^{12} cm^{-2}. This value is comparable to $\sim 10^{12}$ cm^{-2} hole density typically observed in electrically contacted graphene on SiO_2.[4,5] While thermal removal of hole doping effects arising from ambient oxygen molecules with the aid of the oxide substrate has been reported previously,[20,21] confirmation using simultaneous electrical and Raman measurements has not. We note that freshly cleaved graphene samples from HOPG on clean SiO_2/Si substrates typically exhibit significantly upshifted G-band frequencies (>1585 cm^{-1}), indicating that they are already significantly hole doped even prior to device fabrication and annealing.

Figure 2b inset shows that heating to 560 K and cooling back to room temperature under Ar (and measuring under Ar) led to improved device performance. Both the maximum and the minimum in the conductance increase. More importantly, the field-effect mobilities of both electrons and holes increase by about an order of magnitude to 2200 and 2500 cm^2 V^{-1} s^{-1}, respectively. The filled circles in Figure 3 show how the conductance of the graphene device at $V_g = 0$ V changes during the first heating cycle. Initially, there is a slight decrease in the conductance followed by a sharp increase at $T > 400$ K. Upon heating for the second time under Ar, a different trend is seen where the conductance (measured at V_g corresponding to the DP) increases approximately linearly with increasing T as expected based on results of refs 22 and 23.

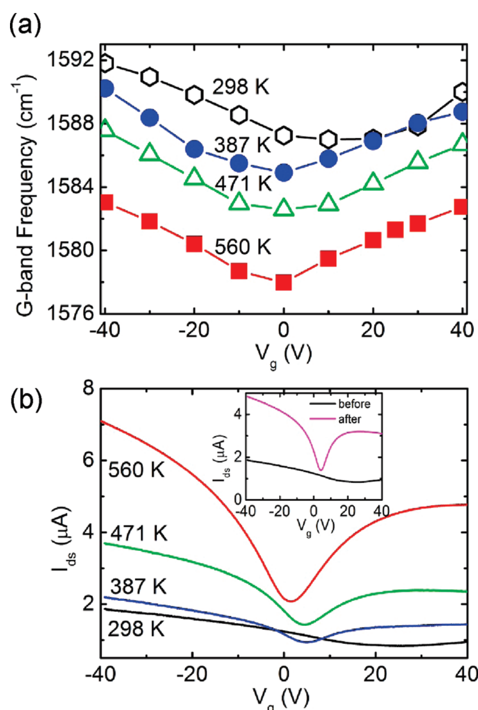

Figure 2. Gate dependence of G-band frequency (a) and the corresponding transfer characteristics (b) at the indicated temperatures during the initial heating cycle. In all cases, drain–source current (I_{ds}) is measured with an applied bias of 10 mV. Room-temperature transfer characteristics before and after the first heating cycle are shown in the inset of (b).

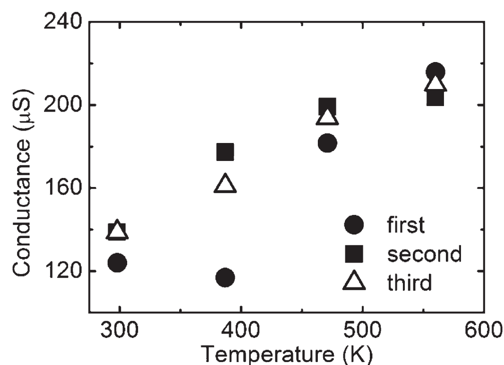

Figure 3. Electrical conductance at gate voltage $V_g = 0$ V during the first (circles), second (squares), and third (open triangles) heating cycles. With the exception of first heating cycle room-temperature data point, $V_g = 0$ V corresponds to the Fermi level position being near DP in all cases.

A convergent behavior is seen upon heating for the third time. The initial deviation in the temperature dependence of the conductance during the first heating cycle is consistent with the removal of hole doping effects;[20] that is, initial heating causes the graphene to be charge neutral and hence the reduction in conductance. However, the conductance rise at $T > 400$ K being steeper than second and third heating cycles, despite the fact that all cycles at these temperatures have the Fermi level near the DP, suggests additional effects due to thermal desorption of ambient molecular species,

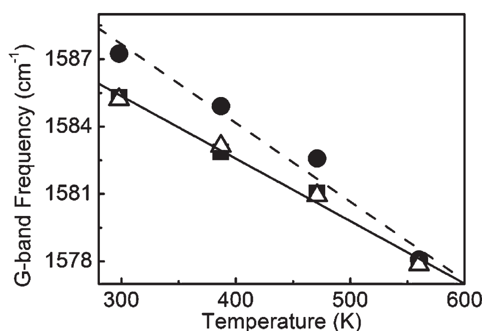

Figure 4. Temperature dependence of G-band frequency at $V_g = 0$ V during the first (circles), second (filled squares), and third (open triangles) heating cycles. Lines are linear curve fits.

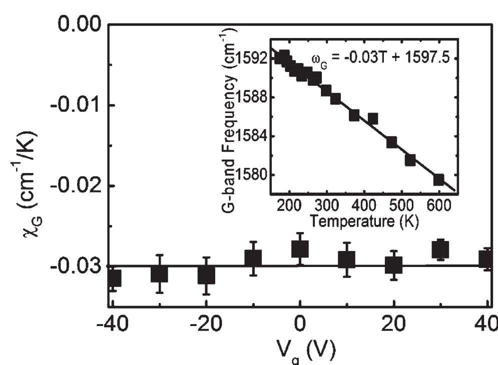

Figure 5. First-order temperature coefficient of G-band frequency (χ_G) measured at different gate voltage V_g. Temperature dependence of G-band frequency of a graphene sample without electrical contacts is shown in the inset with the line representing linear curve fit.

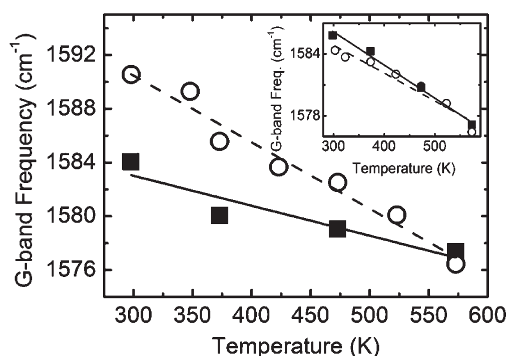

Figure 6. Temperature dependence of G-band frequency during the first heating cycle of two graphene samples exhibiting different initial frequencies. Lines are linear curve fits. Larger initial G-band frequency leads to larger slope (*i.e.*, larger temperature coefficient, χ_G) mainly due to removal of hole doping effects. During the second heating cycle, χ_G converges to ~ -0.03 cm^{-1}/K for both samples (inset).

changes in interactions with the substrate, and/or changes in the contacts.

The G-band frequency shift with V_g also shows similar differences between initial and subsequent heating cycles. The temperature dependent G-band shift at $V_g = 0$ V is shown in Figure 4. The initial heating from 298 to 560 K leads to G mode downshift of 9.5 cm^{-1}, whereas second and subsequent heating cycles lead to a downshift of only 7.5 cm^{-1}. Quantifying this temperature dependent G-band frequency shift has been important especially in measuring graphene thermal conductivity and studying electrical power dissipation in graphene devices.[3,7,9,19] Within a finite temperature range, the temperature dependence of G-band frequency can be estimated to be linear: $\omega(T) = \omega_0 + \chi_G T$, where ω_0 is the G-band frequency in the zero-temperature limit and χ_G is the first-order temperature coefficient.[8] Linear fits to data in Figure 4 give $\chi_G = -0.035 \pm 0.002$ cm^{-1}/K and $\chi_G = -0.028 \pm 0.002$ cm^{-1}/K for the first and subsequent heating cycles, respectively. This difference can again be attributed to the removal of hole doping effects during initial heating as confirmed by the electrical data in Figure 3 and indicates the importance of ensuring fixed Fermi level position in evaluating temperature dependence of the G-band optical phonon energy. The zero gate voltage G-band frequency values of 1587 cm^{-1} at room temperature prior to first heating cycle and 1585 cm^{-1} at the beginning of second heating cycle correspond to hole density decrease of 1.4×10^{12} cm^{-2} based on the DP shift of 20 V obtained simultaneously during the Raman measurements. This change in hole density is consistent with a previous report where $\sim 10^{12}$ cm^{-2} change in carrier density has been shown to lead to ~ 2 cm^{-1} change in G-band frequency.[5]

Figure 5 shows χ_G at different V_g extracted from the second heating cycle when deviations from expected behavior due to removal of ambient hole doping effects have been removed. The temperature coefficient of ~ -0.03 cm^{-1}/K is independent of V_g. Although the degree of electron–phonon coupling-induced softening, especially at Fermi level positions of half the G-band phonon energy above and below the DP where the phonon energy minima are expected, should be temperature dependent,[4,11] we do not observe differences in χ_G at these regions in the relatively high temperature range studied here. The inset in Figure 5 shows the G-band shift over a larger temperature range from 598 to 173 K for a graphene sample without electrical contacts and therefore without potential contamination from fabrication steps. The linear fit gives the same result of $\chi_G = -0.030 \pm 0.002$ cm^{-1}/K. This sample was annealed at 598 K under Ar for 1 h prior to cooling to remove complications arising from varying doping level with temperature and the fixed Fermi level position (expected to be near the DP) is ensured by a constant integrated G/2D intensity ratio.[6] Although the softening of the G-band phonon mode is strongly dependent on the Fermi level position, the change in the phonon energy with temperature is expected to be dominated by anharmonic processes.[17] Results shown in Figure 5 confirm this expectation and indicate that the anharmonic coupling is unaffected by changes in the Fermi level position.

Hence, as long as the measurements are carried out at a fixed Fermi level position, the temperature coefficient χ_G remains independent of which Fermi level position is chosen.

The value of χ_G reported in the literature varies widely from about −0.016 to −0.073 cm^{-1}/K.[8,18,21,24−27] One possible reason for the variation can be the differences in the temperature range studied as G-band frequency shift can only be approximated as linear in a finite temperature range. However, χ_G = −0.016 cm^{-1}/K reported by Calizo *et al.*[8,28] is substantially different than our results in Figure 5 inset, although there is a significant overlap in the temperature range studied (*i.e.*, 83 to 373 K in refs 8 and 28 compared to 173 to 600 K in Figure 5 inset). Much of the large difference may be better attributed to different starting materials with different degrees of disorder and possibly different chemical composition (*i.e.*, mechanically cleaved natural graphite/HOPG, reduced from chemically exfoliated graphite oxide, or CVD grown). However, even within mechanically cleaved graphene samples without detectable D-band, which usually exhibit the highest electrical performance, there is a significant variation in χ_G.[8,21,26] To examine this discrepancy further, we compare in Figure 6 the first heating cycle temperature dependence of two graphene samples that exhibit different initial G-band frequencies. One sample has starting G-band frequency of 1584 cm^{-1} and exhibits χ_G = −0.022 ± 0.002 cm^{-1}/K. Another sample with initial high G-band frequency of 1591 cm^{-1} shows a significantly more negative χ_G of −0.050 ± 0.003 cm^{-1}/K. As shown in the inset, upon the second heating cycle, both exhibit similar χ_G values (−0.030 ± 0.002 cm^{-1}/K for the first sample with lower initial G-band frequency and −0.027 ± 0.002 cm^{-1}/K for the second sample as shown in the inset). On the basis of our results above on electrically contacted graphene, we attribute the large difference in χ_G of the two samples during the first heating cycle mainly to differences in initial degree of doping. Given the results of ref 20, where combined scanning tunneling microscopy and Raman studies have shown interactions with SiO_2 substrates to lead to subnanometer structural deformations upon annealing, we anticipate that the least negative value of χ_G = −0.022 cm^{-1}/K is closer to the intrinsic value. However, most graphene devices are often deposited on Si/SiO_2 substrates and require annealing to ensure high electrical performance. Furthermore, many graphene samples exhibit G-band frequencies significantly up-shifted from a charge neutrality value of ∼1580 cm^{-1} even without annealing, suggesting strong interaction with the oxide substrate to be already present. Therefore, χ_G value of −0.03 cm^{-1}/K appears to be the relevant value for most graphene samples especially those incorporated into devices fabricated on SiO_2 substrates.

While very large negative values of χ_G may be attributed to initial heating induced removal of hole doping effects, χ_G = −0.03 cm^{-1}/K we report here is

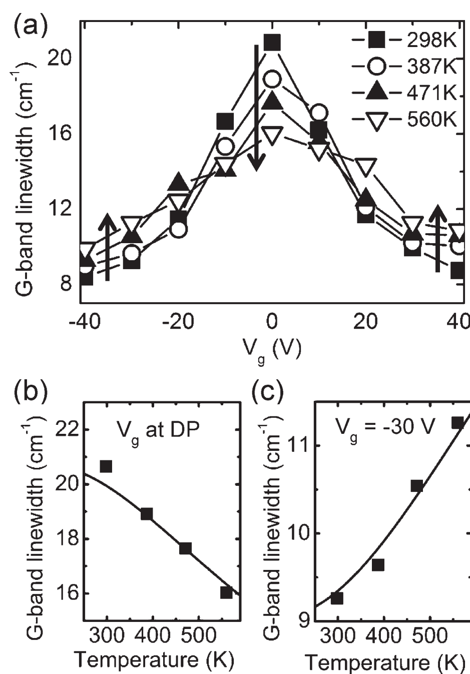

Figure 7. (a) Gate dependence of G-band line width at indicated temperatures. The arrows emphasize the opposite temperature dependences at different Fermi levels. (b) Temperature dependence of G-band line width at charge neutral state. Solid line is a fit to temperature dependence given in ref 17. (c) Temperature dependence of G-band line width at V_g = −30 V where Fermi level is well below the DP. Solid line is a curve fit to simple decay of optical phonon into two acoustic phonons.[10]

obtained when the doping level is ensured to be fixed with applied gate voltage. Then, there must be some other mechanism responsible for the permanent change in the *T* response. The two main contributions to *T* dependence of G-band frequency and therefore to χ_G are anharmonic coupling and lattice thermal expansion.[17] The anharmonic coupling of optical phonons to lower energy phonons leads to a decrease in G-band frequency with temperature, whereas the lattice expansion term leads to an increase due to the negative coefficient of thermal expansion of graphene. The more negative value of χ_G observed upon the second heating cycle for the sample with lower initial G-band frequency may then be explained by the enhanced interaction with the substrate. That is, due to the strong interaction with the substrate, which has a positive coefficient of thermal expansion, contraction of the graphene lattice with increasing temperature becomes less likely. This thermally induced strain in turn reduces the lattice thermal expansion contribution to χ_G, making it more negative.

In contrast to the G-band frequency, the temperature dependence of the G-band line width at Fermi level position near the DP is dominated by electron−phonon coupling rather than anharmonic decay.[17] Figure 7a shows the dependence of G-band line width on V_g at the indicated temperatures. While the line

broadening near the DP occurs at all temperatures, the degree of broadening decreases and the gate dependence profile broadens with increasing temperature. With the Fermi level near the DP, the line width exhibits a decrease with temperature rise, as shown in Figure 7b. This temperature dependent G-band line width is fitted using eq 2 of ref 17, and the only fitting parameter is the zero-temperature line width. Good agreement with the theoretical prediction verifies that the electron−phonon coupling dictates the temperature dependence of the line width. On the other hand, when the applied V_g shifts the Fermi level away from the DP, phonon−phonon interactions, rather than the electron−phonon coupling, become more important, as evidenced in Figure 7c, where the G-band line width (at V_g = −30 V) now has an opposite trend of increasing with temperature. The line is a fit to a simple expression for optical phonon decay into two acoustic phonons as given in ref 10. The only fitting parameter here again is the zero-temperature line width.

We note that the G-band line width near the DP at room temperature increases irreversibly with annealing. The maximum G-bandwidth increases from 18 to 21 cm^{-1} upon the first annealing cycle. Since we apply gate voltage to ensure the Fermi level to be near the DP, the broadening cannot be due to doping effects altering electron−phonon coupling. The increased line width is consistent with inhomogeneous broadening caused by structural deformations due to enhanced interactions with the substrate.[20] If this is indeed true, then the G-band line width at the DP may be more sensitive to such small deformations than the D-band, which is not detectable in our graphene samples as well as in samples in ref 20. This may also explain significantly larger values (∼20 cm^{-1}) of G-band line width often reported than the theoretical value of ∼13 cm^{-1}.[17]

Finally, we discuss temperature dependence of Raman 2D mode at different gate voltages. Figure 8a shows the gate dependence of 2D peak position at the indicated temperatures for the first and the second heating cycles. There appears to be a slight softening at all temperatures examined, but the magnitude of the downshift is only about half of that observed for the G-band. Similar to the electrical conductance and the G-band features, the 2D-band exhibits different behavior in the first heating cycle but second and third cycles show convergent behavior. The first-order temperature coefficient of the 2D mode χ_{2D} is -0.050 ± 0.003 cm^{-1}/K for the second and third heating cycles (Figure 8b) and is also independent of gate voltage. Much like the G-band, the 2D mode exhibits larger downshift with temperature during the first heating cycle and the corresponding initial χ_{2D} is −0.077 cm^{-1}/K. However, this difference cannot be accounted for by the removal of hole doping effects upon initial heating. First, the data shown in Figure 8b are at V_g corresponding to the DP (as ascertained by concurrent G-band frequency

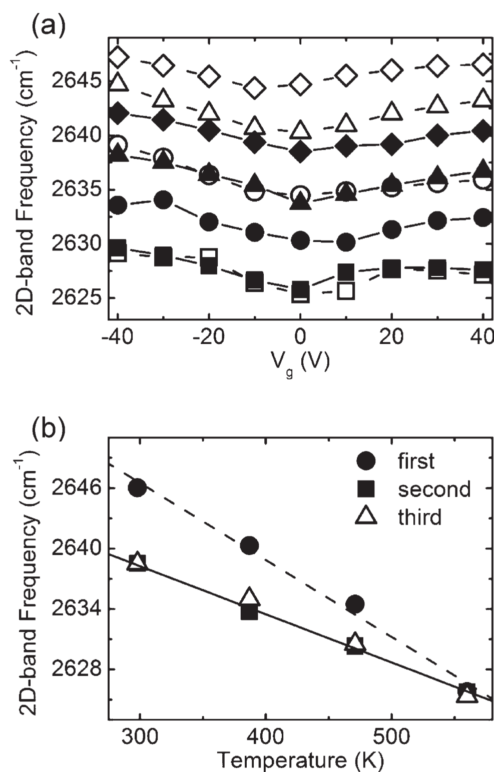

Figure 8. (a) Gate voltage dependence of 2D-band frequency during the first (open symbols) and second (closed symbols) heating cycles. Corresponding temperatures are 298, 387, 471, and 560 K from top to bottom for both cycles. (b) Temperature dependence of 2D-band frequency at the DP during the first (circles), second (filled squares), and third (open triangles) heating cycles.

and electrical conductance minima). Furthermore, the maximum gate-induced 2D frequency shift is only ∼2 cm^{-1}, which will lead to maximum change in χ_{2D} of −0.008 cm^{-1}/K. The actual change observed is −0.027 cm^{-1}/K, which is more than 3 times the maximum change expected. We note that the 2D-band frequency at the DP at 298 K decreases from 2646 to 2639 cm^{-1} upon initial heating, as seen in Figure 8b. This difference in room-temperature 2D frequency at the DP may be associated with changes in the interactions with the substrate which can in turn alter χ_{2D}. While the weak V_g dependence (at least near the DP) as well as a larger first-order temperature coefficient may make the 2D-band frequency appear to be a better indicator of temperature, these possible complications that are not associated with doping need to be better understood first. However, given that 2D-band is very sensitive to interlayer interactions,[30] even van der Waals interactions with the substrate may affect the 2D mode frequency.

The 2D-band line width is independent of V_g but does broaden slightly with increasing temperature (∼2 cm^{-1} increase from 298 to 560 K with initial width of 30 cm^{-1}). This slight increase in width is also independent of V_g. Unlike the G-band, there is no significant broadening of the 2D-band near the DP at 298 K before and after the first heating cycle. However, as

mentioned above, the 2D frequency near the DP downshifts irreversibly by 7 cm^{-1} upon heating and cooling back to room temperature, which may be associated with changes in interactions with the substrate.

CONCLUSIONS

By a combination of Raman and electrical measurements, we have shown gate dependent Raman spectra of single-layer graphene at a temperature range of 298 to 560 K. Changes in the conductance and the G-band mode spectral features upon initial heating of samples equilibrated in air indicate removal of hole doping effects. Thermal removal of these doping effects, which have been shown to arise from molecular oxygen adsorption and interactions with the SiO_2 substrates,[20,21] can lead to variations in the first-order temperature coefficients of both G- and 2D-band frequencies. Although our results suggest that the intrinsic temperature coefficient χ_G may be closer to ~ -0.02 cm^{-1}/K, $\chi_G = -0.03$ cm^{-1}/K appears to be the more relevant number for single-layer graphene devices fabricated on SiO_2. However, irreversible changes in χ_G, χ_{2D}, G-band line width, and 2D-band frequency in the zero-charge limit for graphene on SiO_2 are observed, which cannot be accounted for by doping level changes upon heating. The more negative value of χ_G in the absence of a detectable D-band may be explained by strong interactions with the substrate that reduce the contribution of lattice thermal expansion. Both χ_G and χ_{2D} remain constant at all gate voltages examined here, indicating that as long as the Fermi level position is fixed these coefficients remain independent of which Fermi level position is chosen. In contrast, the G-band line width is strongly affected by the electron−phonon coupling and therefore strongly dependent on the doping level. Increasing line width with increasing temperature is seen near the DP, whereas the opposite trend is observed at large gate voltages (away from the DP) where phonon−phonon interactions rather than electron−phonon coupling become the dominant term. Upon initial heating under Ar, we also observe that the room-temperature maximum G-band line width near the DP increases irreversibly possibly due to inhomogeneous broadening induced by interactions with the substrate.

METHODS

Graphene samples were prepared by micromechanical cleavage[29] of highly oriented pyrolytic graphite (HOPG, SPI Supplies, grade SPI-1) on Si substrates with a 300 nm thick thermal oxide layer. Single-layer graphene flakes were identified by their color under an optical microscope and confirmed by their Raman 2D-bands. A single, sharp Lorentzian 2D feature ($\sim<$ 30 cm^{-1} full width at half-maximum) confirms that all measurements were performed on single layers.[30] Metal contacts (40 nm of Au with 3 nm of Ti wetting layer) were deposited by conventional photolithography. After fabrication, graphene devices were annealed at 350 °C for 1 h under 1:1 Ar/H_2 flow at 600 cm^3/min to remove residual photoresist[31,32] and equilibrated in air prior to measurements. Measurements with varying temperature were carried out in an airtight heating stage with gas inlet/outlet and electrical feedthroughs. Electrical measurements were carried out at a low bias of 10 mV to ensure Joule heating/non-equilibrium effects do not contribute to the observed temperature dependence.[19] All temperature dependent measurements were carried out under 20 cm^3/min Ar flow. Prior to measurements, samples were allowed to equilibrate at least 20 min after each temperature of interest was reached. Raman spectra were acquired on a Jobin Yvon Labram HR800 micro-Raman spectrometer with 633 nm laser excitation and a 100× long working distance air objective (laser spot size $\sim$1 μm). Laser intensity was kept below 1 mW to ensure that laser-induced heating effects did not complicate the results obtained. Both the G- and the 2D-bands are fitted to a single Lorentzian for analysis. All line widths given are full width at half-maximum.

Acknowledgment. This material is based upon work supported in part by the NSF (Grant No. 09-05175). Experiments were carried out in part in the Frederick Seitz Materials Research Laboratory Central Facilities, University of Illinois.

REFERENCES AND NOTES

1. Castro Neto, A. H.; Guinea, F.; Peres, N. M. R.; Novaslov, K. S.; Geim, A. K. The Electronic Properties of Graphene. *Rev. Mod. Phys.* **2009**, *81*, 109–162.
2. Du, X.; Skachko, I.; Barker, A.; Andrei, E. Y. Approaching Ballistic Transport in Suspended Graphene. *Nat. Nanotechnol.* **2008**, *3*, 491–495.
3. Balandin, A. A.; Ghosh, S.; Bao, W.; Calizo, I.; Teweldebrhan, D.; Miao, F.; Lau, C. N. Superior Thermal Conductivity of Single-Layer Graphene. *Nano Lett.* **2008**, *8*, 902–907.
4. Pisana, S.; Lazzeri, M.; Casiraghi, C.; Novoselov, K. S.; Geim, A. K.; Ferrari, A. C.; Mauri, F. Breakdown of the Adiabatic Born−Oppenheimer Approximation in Graphene. *Nat. Mater.* **2007**, *6*, 198–201.
5. Yan, J.; Zhang, Y.; Kim, P.; Pinczuk, A. Electric Field Effect Tuning of Electron−Phonon Coupling in Graphene. *Phys. Rev. Lett.* **2007**, *98*, 166802.
6. Das, A.; Pisana, S.; Chakraborty, B.; Picansec, S.; Saha, S. K.; Waghmare, U. V.; Novoselov, K. S.; Krishnamurthy, H. R.; Geim, A. K.; Ferrari, A. C.; *et al.* Monitoring Dopants by Raman Scattering in an Electrochemically Top-Gated Graphene Transistor. *Nat. Nanotechnol.* **2008**, *3*, 210–215.
7. Ghosh, S.; Bao, W.; Nika, D. L.; Subrina, S.; Pokatilov, E. P.; Lau, C. N.; Balandin, A. A. Dimensional Crossover of Thermal Transport in Few-Layer Graphene. *Nat. Mater.* **2010**, *9*, 555–558.
8. Calizo, I.; Balandin, A. A.; Bao, W.; Miao, F.; Lau, C. N. Temperature Dependence of the Raman Spectra of Graphene and Graphene Multilayers. *Nano Lett.* **2007**, *7*, 2645–2649.
9. Freitag, M.; Steiner, M.; Martin, Y.; Perebeinos, V.; Chen, Z.; Tsang, J. C.; Avouris, Ph. Energy Dissipation in Graphene Field-Effect Transistors. *Nano Lett.* **2009**, *9*, 1883–1888.
10. Chae, D.; Krauss, B.; Klitzing, K. V.; Smet, J. H. Hot Phonons in an Electrically Biased Graphene Constriction. *Nano Lett.* **2010**, *10*, 466–471.
11. Caudal, N.; Saitta, A. M.; Lazzeri, M.; Mauri, F. Kohn Anomalies and Nonadiabaticity in Doped Carbon Nanotubes. *Phys. Rev. B* **2007**, *75*, 115423.
12. Zhang, Y.; Xie, L.; Zhang, J.; Wu, Z.; Liu, Z. Temperature Coefficients of Raman Frequency of Individual Single-Walled Carbon Nanotubes. *J. Phy. Chem. C* **2007**, *111*, 14031–14034.
13. Nguyen, K. T.; Gaur, A.; Shim, M. Fano Lineshape and Phonon Softening in Single Isolated Metallic Carbon Nanotubes. *Phys. Rev. Lett.* **2007**, *98*, 145504.

14. Casiraghi, C.; Pisana, C. S.; Novoselov, K. S.; Geim, A. K.; Ferrari, A. C. Raman Fingerprint of Charged Impurities in Graphene. *Appl. Phys. Lett.* **2007**, *91*, 233108.
15. Kalbac, M.; Reina-Cecco, A.; Farhat, H.; Kong, J.; Kavan, L.; Dresselhaus, M. S. The Influence of Strong Electron and Hole Doping on the Raman Intensity of Chemical Vapor-Deposition Graphene. *ACS Nano* **2010**, *4*, 6055–6063.
16. Lazzeri, M.; Mauri, F. Nonadiabatic Kohn Anomaly in a Doped Graphene Monolayer. *Phys. Rev. Lett.* **2006**, *97*, 266407.
17. Bonini, N.; Lazzeri, M.; Marzari, N.; Mauri, F. Phonon Anharmonicities in Graphite and Graphene. *Phys. Rev. Lett.* **2007**, *99*, 176802.
18. Cai, W.; Moore, A. L.; Zhu, Y.; Li, X.; Chen, S.; Shi, L.; Ruoff, R. S. Thermal Transport in Suspended and Supported Monolayer Graphene Grown by Chemical Vapor Deposition. *Nano Lett.* **2010**, *10*, 1645–1651.
19. Berciaud, S.; Han, M. Y.; Mak, K. F.; Brus, L. E.; Kim, P.; Heinz, T. F. Electron and Optical Phonon Temperatures in Electrically Biased Graphene. *Phys. Rev. Lett.* **2010**, *104*, 227401.
20. Ryu, S.; Liu, L.; Berciaud, S.; Yu, Y.-J.; Liu, H.; Kim, P.; Flynn, G. W.; Brus, L. E. Atmospheric Oxygen Binding and Hole Doping in Deformed Graphene on a SiO_2 Substrate. *Nano Lett.* **2010**, *10*, 4944–4951.
21. Abdula, D.; Ozel, T.; Kang, K.; Cahill, D. G.; Shim, M. Environment-Induced Effects on the Temperature Dependence of Raman Spectra of Single-Layer Graphene. *J. Phys. Chem. C* **2008**, *112*, 20131–20134.
22. Vasko, F. T.; Ryzhii, V. Voltage and Temperature Dependencies of Conductivity in Gated Graphene. *Phys. Rev. B* **2007**, *76*, 233404.
23. Shao, Q.; Liu, G.; Teweldebrhan, D.; Balandin, A. A. High-Temperature Quenching of Electrical Resistance in Graphene Interconnects. *App. Phys. Lett.* **2008**, *92*, 202108.
24. Malard, L. M.; Moreira, R. L.; Elias, D. C.; Plentz, F.; Alves, E. S.; Pimenta, M. A. Thermal Enhancement of Chemical Doping in Graphene: A Raman Spectroscopy Study. *J. Phys: Condens. Matter* **2010**, *22*, 334202.
25. Allen, M. J.; Fowler, J. D.; Tung, V. C.; Yang, Y.; Weiller, B. H.; Kaner, R. B. Temperature Dependent Raman Spectroscopy of Chemically Derived Graphene. *Appl. Phys. Lett.* **2008**, *93*, 193119.
26. Late, D. J.; Maitra, U.; Panchakarla, L. S.; Waghmare, U. V.; Rao, C. N. R. Temperature Effects on the Raman Spectra of Graphenes: Dependence on the Number of Layers and Doping. *J. Phys: Condens. Matter* **2011**, *23*, 055303.
27. Chen, S.; Moore, A. L.; Cai, W.; Suk, J. W.; An, J.; Mishra, C.; Amos, C.; Magnuson, C. W.; Kang, J.; Shi, L.; *et al.* Raman Measurements of Thermal Transport in Suspended Monolayer Graphene of Variable Sizes in Vacuum and Gaseous Environments. *ACS Nano* **2011**, *5*, 321–328.
28. Calizo, I.; Miao, F.; Bao, W.; Lau, C. N.; Balandin, A. A. Variable Temperature Raman Microscopy as a Nanometrology Tool for Graphene Layers and Graphene-Based Devices. *Appl. Phys. Lett.* **2007**, *91*, 071913.
29. Novoselov, K. S.; Geim, A. K.; Morozov, S. V.; Jiang, D.; Dubonos, S. V.; Girgorieva, I. V.; Firsov, A. A. Electric Field Effect in Atomically Thin Carbon Films. *Science* **2004**, *306*, 666–669.
30. Ferrari, A. C.; Meyer, J. C.; Scardaci, V.; Casiraghi, C.; Lazzeri, M.; Mauri, F.; Piscanec, S.; Jiang, D.; Novoselov, K. S.; Roth, S.; *et al.* Raman Spectrum of Graphene and Graphene Layers. *Phys. Rev. Lett.* **2006**, *97*, 187401.
31. Ishigami, M.; Chen, J. H.; Cullen, W. G.; Fuhrer, M. S.; Williams, E. D. Atomic Structure of Graphene on SiO_2. *Nano Lett.* **2007**, *7*, 1643–1648.
32. Romero, H. E.; Shen, N.; Joshi, P.; Gutierrez, H. R.; A. Tadigadapa, S.; Sofo, J. O.; Eklund, P. C. n-Type Behavior of Graphene Supported on Si/SiO_2 Substrates. *ACS Nano* **2008**, *2*, 2037–2044.